Manipulation of Subsurface Donors in ZnO

Hao Zheng,* Alexander Weismann, and Richard Berndt

Institut für Experimentelle und Angewandte Physik, Christian-Albrechts-Universität zu Kiel, D-24098 Kiel, Germany

(Received 26 February 2013; revised manuscript received 17 April 2013; published 28 May 2013)

Single donors close to the ZnO(0001) surface are investigated with scanning tunneling microscopy. Their binding energies and depths are determined from spatially resolved spectra of the differential conductance. At elevated bias of the STM tip, vertical motion of the donors can be induced. The direction of the motion can be controlled by the bias polarity.

DOI: 10.1103/PhysRevLett.110.226101 PACS numbers: 68.37.Ef, 66.30.−h, 71.55.Gs, 85.30.Fg

The capability to manipulate structures at the atomic scale is an important asset of the scanning tunneling microscope (STM). Nowadays atoms may be arranged on metal and semiconductor surfaces as well as thin insulating films into nanostructures [1–7]. Single molecules may be modified and chemical reactions may be induced [8–11]. Usually this exquisit control is limited to the surface. A recent exception is H in Pd, which could be moved with a STM tip [12]. No comparable results have been reported for semiconductors or insulators where the controlled positioning of subsurface dopants would be desirable.

Here we present the manipulation of interstitial Zn (Zn_I) in ZnO, a semiconductor with extraordinary electronic, optical, and chemical properties [13]. Zn_I is a shallow donor and has been suggested to lead to the *n*-type conductance of ZnO [14,15]. We show that the STM tip can push and pull subsurface donors.

Controlling the diffusion of cations is important for oxide-based resistive switches, which have potential applications as nonvolatile memories [16]. Resistive switching has been reported from ZnO-based Schottky contacts that relied on the diffusion of cations from metal electrodes [17,18]. The positioning of a single dopant in our experiment represents a particularly small implementation of a resistive switch. Similar to a Schottky contact, an Au tip induces upward bending of the ZnO bands. Resistive switching is achieved by manipulation of a donor. As a side effect, the binding energy E_b of the donor also changes.

The ZnO(0001) crystals (Mateck, Germany) we used displayed a light yellow color. After cycles of Ar^+ bombardment and annealing to ≈700 °C in ultrahigh vacuum, the samples were transferred *in vacuo* to a STM operated at 5 K. Tips were cut from Au wire, annealed, and brought into contact with the ZnO surface. The bias voltage V was applied to the sample, and a lock-in amplifier (modulation 15–30 mV_{rms}) was used to measure the differential conductance (dI/dV).

On a nm scale, the ZnO(0001) surface is not atomically flat, owing to its polar nature [19]. In addition, inhomogeneities at or near the surface cause irregular variations of the apparent height and thus mask the effect of the donors in topographs. Taking advantage of the increased energy resolution of dI/dV maps, donors may nevertheless be resolved [15]. Bright rings can be discerned in these maps [Fig. 1(a)], which indicate transitions of the charge state of a Zn_I donor below the ZnO(0001) surface [20]. The lateral tip position determines the tip-induced band bending (TIBB) at the donor, which is located near the center of the rings. The donor of Fig. 1(a) is neutral when the STM tip is outside of the rings, becomes singly charged when the tip is crossing the outer ring, and finally is doubly charged

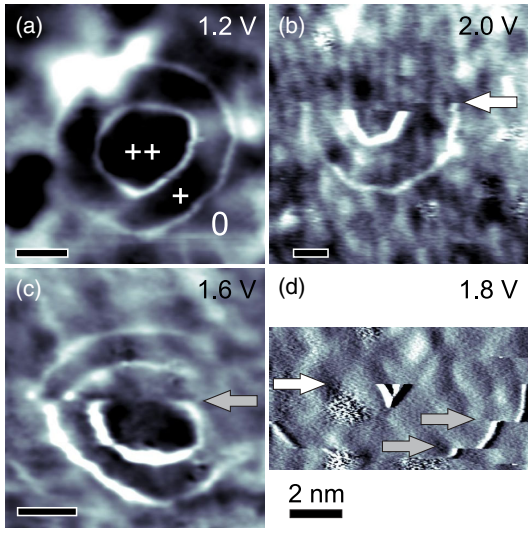

FIG. 1 (color online). dI/dV maps from four different donors on ZnO(0001) recorded at $I = 1$ nA. White indicates high conductance. The slow scanning direction was from bottom to top. Scale bars correspond to 2 nm. (a) At low V two concentric rings of increased conductance are observed. The rings signal the ionizations of a subsurface donor at their center. 0, +, and ++ indicate its charge states. (b) At more elevated voltage, rings that are observed in the initial scan lines suddenly disappear (arrow). (c) The diameters of two ionization rings increase within the indicated scan line. Moreover, the signal contrast is diminished. (d) A single ionization feature at the bottom of the image repeatedly increases in diameter (gray arrows) until it finally disappears (white arrow). The contrast in (d) has been enhanced by differentiation along the horizontal direction.

inside the inner ring. A positive donor lowers the electrostatic potential experienced by tunneling electrons and thus increases the current. In dI/dV maps this leads to a sharp ring of increased conductance.

While the ionization rings of Fig. 1(a) could be reproducibly imaged at $0 < V < 1.2$ V, permanent changes are induced at larger V. Figure 1(b) shows an example. In the dI/dV map, which was recorded from bottom to top at $V = 2.0$ V, two concentric ionization rings were initially observed but disappeared during the scan line marked by a white arrow. Figure 1(c) displays another typical result. In the upper half of the image, the ring diameters are larger and the corresponding contrast is reduced. Finally, Fig. 1(d) shows a case where the diameter of a single ring increases twice. Larger maps show that single donors may be manipulated without significantly affecting their neighbors (see Supplemental Material [21]). Therefore the observed modifications cannot be due to changes of the tip apex. The conditions for inducing manipulation of a particular donor exhibited scatter, presumably due to inhomogeneities of the surface and the influence of nearby donors.

Next, I-V curves were recorded at positive V [Fig. 2(a)]. Charging occurs at 0.24 V $(0/+)$ and 0.93 V $(+/++)$, where the tunneling current abruptly rises [15,22]. The current drop by $\approx 40\%$ at $V_m \approx 1.17$ V is a new feature. V_m varied between different donors. At the opposite polarity, changes occurred at larger voltages. In the voltage range from -2 to -3 V of Fig. 2(c), the donor is neutral.

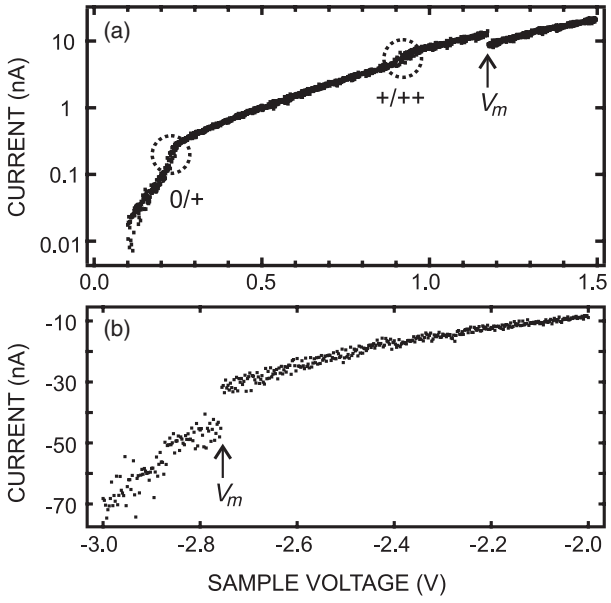

FIG. 2. I-V curves recorded above a donor at (a) positive and (b) negative voltage. (a) Logarithmic and (b) linear scales are used for clarity. $0/+$ and $+/++$ indicate ionizations of the donor from neutral to positive and from singly to doubly charged. At the voltages labeled V_m, permanent transitions occur. The set point before opening the current feedback was 1 nA and 0.5 V.

Nevertheless, an abrupt 40% rise of the current occurred at $V_m \approx -2.75$ V. dI/dV maps recorded before and after manipulation at negative voltage revealed that the size of the ionization rings had decreased, which is opposite to the positive voltage case.

These manipulations may be combined to move a donor up and down (Fig. 3). The close correspondence of the charging pattern (bright lines surrounding the donor) before and after the cycle demonstrates the reversibility of the process. For some donors this cycle was repeated four times.

Figure 4 shows dI/dV spectra represented by false colors from positions close to and above a donor (a) before and (b) after manipulation along with (c) a single spectrum. The maps exhibit two parabolic conductance maxima (black dotted lines), which are due to ionization processes. The variation of the ionization peaks with lateral position reflects the change of the TIBB at the donor. To pull an occupied level above E_F, a small positive voltage is required when the donor is right below the tip. This voltage increases at larger separations [22]. The parabolae at negative V are due to empty levels that are pushed below E_F. This requires the contact potential, which is maximal below the tip, be compensated. The voltage $|V|$ for ionization therefore is largest for a donor below the tip apex [23]. The defect levels D^0 and D^+ are also discernible in the maps. Their curvatures are opposite to those of the ionization parabolae and replicate the shape of the TIBB [23,24]. The corresponding vibrational excitations display similar shapes.

We used Feenstra's Poisson equation solver [25] to model the experimental data. A number of parameters are required. The band gap at 5 K of 3.4553 eV and a ZnO dielectric constant of 7.88 were taken from Refs. [26,27]. The tip-sample distance was estimated to 0.5 nm by contacting the sample. Moreover, we used a tip apex radius of 1 nm and a shank angle of 30°. From the Au work function [28,29] and the ZnO electron affinity [30],

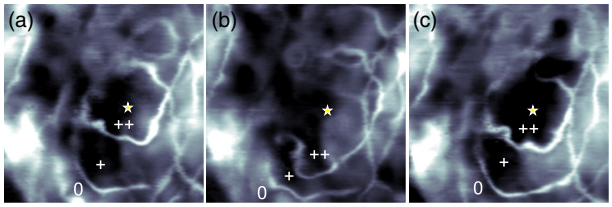

FIG. 3 (color online). Series of dI/dV maps from a donor that is located approximately at the position marked by an asterisk [(12 nm)^2, 0.8 V, 1 nA]. (a) Before manipulation two charging rings can be discerned around the donor. 0, +, and ++ mark the charge states of the donor for the respective lateral distances of the tip. (b) After pushing the donor deeper into the crystal using $V = 1.4$ V and $I = 42.6$ nA, the ring diameters have increased. (c) After pulling the donor back towards the surface with $V = -2.8$ V and $I = 26$ nA, the initial state is restored except for small variations in the vicinity.

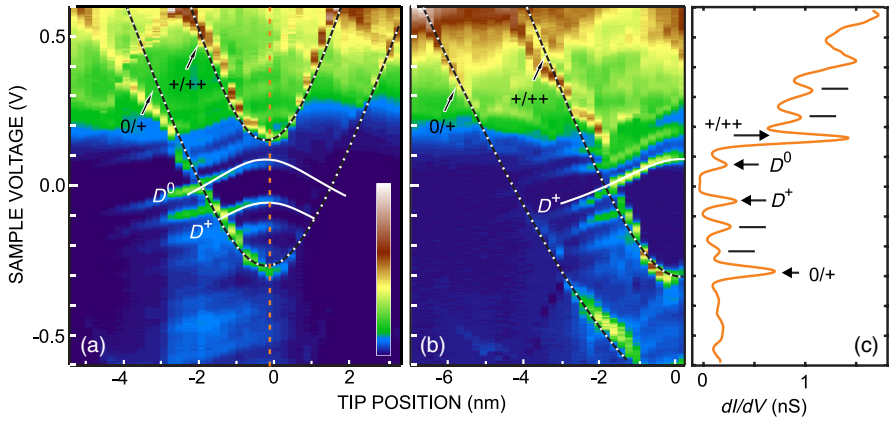

FIG. 4 (color online). False-color map of dI/dV spectra of a donor located at position zero (a) before and (b) after manipulation at 1.5 V and 1 nA. The STM feedback was disabled at 0.6 V and 3 nA. The color bar corresponds to (a) 0–2.5 nS and (b) 0–2.1 nS. Dotted parabolae represent the results of model calculations of the variation of the ionization threshold. Solid lines indicate the calculated levels of the neutral (D^0) and singly charged (D^+) donor. Vibronic transitions cause additional maxima that run in parallel to the donor levels. Depending on voltage and tip position the donor is neutral below the parabola labeled $0/+$, singly charged between parabolae, or doubly charged above the parabola labeled $+/++$. (c) dI/dV spectrum indicated by a vertical dashed line in (a). In addition to the ionization peaks ($0/+$, $+/++$), the donor levels D^0 and D^+ may be discerned along with a series of vibronic peaks (bars).

we estimate a contact potential of 1.3 eV. Consistent with Hall data [31], a donor density of 2×10^{18} cm^{-3} was used.

We varied the levels D^0 and D^+ and the depth of the donor below the surface to optimize the fit of the seven curves indicated in Fig. 4. The calculated results match the experimental data rather well, although some irregular deviations are not reproduced. The simulation places the donor 0.2 nm [$\sim$1 monolayer (ML)] below the surface. The binding energies prior to manipulation [230 meV (D^0) and 340 meV (D^+)] decreased to 105 and 190 meV, respectively, and the depth increased to 0.45 nm (2 ML). Similar fits may be obtained for slightly different parameters. However, the fits consistently showed an increase of the depth and reduced binding energies. A similar depth-related reduction of the binding energy has been reported from dopants in GaAs [32,33].

After manipulation the opening of the parabolae in Fig. 4 is wider, which corresponds to larger rings in dI/dV maps. Moreover, the contrast of the dI/dV signal is reduced, which further confirms that a donor is pushed into the crystal [34]. Contrast reduction below the detection limit may also explain the disappearance of rings [Figs. 1(b) and 1(d)]. Alternatively, the donor levels may be shifted into the conduction band of the ZnO bulk [35]. Such a donor would be doubly charged at any voltage, and no ionization features would be observed.

Next, the resistive switching observed in Fig. 2 is discussed. To push a donor into the crystal, positive V were used [Fig. 2(a)]. Concomitantly, the binding energy is reduced and the conductance decreases. In a macroscopic semiconductor, a lower binding energy would reduce the resistance at low temperatures. The resistance increase observed here may be understood as follows. At $V > 0$, the ZnO bands are bent upwards. From the charging transitions in Fig. 2(a), it is clear that the donor is doubly charged throughout the manipulation process. Its Coulomb field reduces the band bending and facilitates electron injection into the ZnO conduction band. As the donor is pushed away from the surface, this effect diminishes and the current drops. In contrast, at $V < 0$, the current is due to electrons from the conduction band and from the neutral donor. Manipulation at this polarity pulls the donor toward the surface, reduces the donor-tip distance, and increases the current [Fig. 2(b)].

Presently, the mechanism of the manipulation process is not clear. At $V > 0$, donors move inward, opposite to the direction of the electrostatic force exerted by the tip, but in line with the electron momentum. Nevertheless, momentum exchange between electrons and the donor (electron wind force [36]) is not likely to be the only driving force. The wind force is expected to be proportional to the local current density [37]. However, at low voltage, $V = 0.5$ V, no donor motion was observed despite elevated currents up to 10 nA. To induce motion, V had to be increased to at least 1.1 V. The injection of hot electrons at elevated bias causes multiple vibrational excitation, cf. Fig. 4(c). We tentatively suggest that this induces diffusion of the donor similar to the case of H in Pd [38]. Density-functional calculations showed that the diffusion barrier of Zn_I in Zn chalcogenides and oxides decreases upon charging [39] and is $\approx$500 meV in the doubly charged state in ZnO [35]. In dI/dV spectra, we observed up to fivefold vibrational excitation of a mode with an energy of $\approx$ 60–76 meV. Excitation of higher harmonics would suffice to overcome the diffusion barrier. While such processes may be too rare for detection in dI/dV they are likely to occur on the time scale of the manipulation experiments. The different charge states of the donors at

positive and negative bias may also underlie the different manipulation thresholds observed. A related effect has been observed for Zn_I in ZnSe, where optical excitation was found to enable diffusion at low temperature [40].

In summary, we presented STM-based manipulation of donors in ZnO. Donor motion from and to the surface can be controlled by the polarity of the tip voltage. Simultaneously, with the vertical motion the binding energy of the donors changes and the conductance of the tunneling junction is modified, turning the buried donor into a resistive switch. Given that resistive switching via impurity diffusion has often been reported, the vertical manipulation demonstrated for ZnO may presumably be used for a range of materials.

H. Z. thanks R. M. Feenstra for advice on using his software. Financial support by the Deutsche Forschungsgemeinschaft through SFB 855 is acknowledged.

*zheng@physik.uni-kiel.de

[1] J. A. Stroscio and D. M. Eigler, Science **254**, 1319 (1991).
[2] T.-C. Shen, C. Wang, G. C. Abeln, J. R. Tucker, J. W. Lyding, Ph. Avouris, and R. E. Walkup, Science **268**, 1590 (1995).
[3] C. F. Hirjibehedin, C. P. Lutz, and A. J. Heinrich, Science **312**, 1021 (2006).
[4] D. Kitchen, A. Richardella, J.-M. Tang, M. E. Flatté, and A. Yazdani, Nature (London) **442**, 436 (2006).
[5] A. K. Khajetoorians, J. Wiebe, B. Chilian, and R. Wiesendanger, Science **332**, 1062 (2011).
[6] N. Néel, R. Berndt, J. Kröger, T. O. Wehling, A. I. Lichtenstein, and M. I. Katsnelson, Phys. Rev. Lett. **107**, 106804 (2011).
[7] J. K. Garleff, A. P. Wijnheijmer, C. N. v. d. Enden, and P. M. Koenraad, Phys. Rev. B **84**, 075459 (2011).
[8] L. Bartels, G. Meyer, K.-H. Rieder, D. Velic, E. Knoesel, A. Hotzel, M. Wolf, and G. Ertl, Phys. Rev. Lett. **80**, 2004 (1998).
[9] S.-W. Hla, L. Bartels, G. Meyer, and K.-H. Rieder, Phys. Rev. Lett. **85**, 2777 (2000).
[10] J. Repp, G. Meyer, S. Paavilainen, F. E. Olsson, and M. Persson, Science **312**, 1196 (2006).
[11] A. Sperl, J. Kröger, and R. Berndt, Angew. Chem. **123**, 5406 (2011).
[12] E. C. H. Sykes, L. C. Fernández-Torres, S. U. Nanayakkara, B. A. Mantooth, R. M. Nevin, and P. S. Weiss, Proc. Natl. Acad. Sci. U.S.A. **102**, 17 907 (2005).
[13] Ü. Özgür, Ya. I. Alivov, C. Liu, A. Teke, M. A. Reshchikov, S. Doğan, V. Avrutin, S.-J. Cho, and H. Morkoc, J. Appl. Phys. **98**, 041301 (2005).
[14] D. C. Look, J. W. Hemsky, and J. R. Sizelove, Phys. Rev. Lett. **82**, 2552 (1999).
[15] H. Zheng, J. Kröger, and R. Berndt, Phys. Rev. Lett. **108**, 076801 (2012).
[16] R. Waser and M. Aono, Nat. Mater. **6**, 833 (2007).
[17] W.-Y. Chang, Y.-C. Lai, T.-B. Wu, S.-F. Wang, F. Chen, and M.-J. Tsai, Appl. Phys. Lett. **92**, 022110 (2008).
[18] Y. C. Yang, F. Pan, Q. Liu, M. Liu, and F. Zeng, Nano Lett. **9**, 1636 (2009).
[19] O. Dulub, U. Diebold, and G. Kresse, Phys. Rev. Lett. **90**, 016102 (2003).
[20] The experiments were focused on near-surface donors, which give rise to small ionization rings. The features from donors in deeper layers are more extended, overlap with those from other defects, and are difficult to analyze.
[21] See Supplemental Material at http://link.aps.org/supplemental/10.1103/PhysRevLett.110.226101 for [brief description].
[22] K. Teichmann, M. Wenderoth, S. Loth, R. G. Ulbrich, J. K. Garleff, A. P. Wijnheijmer, and P. M. Koenraad, Phys. Rev. Lett. **101**, 076103 (2008).
[23] A. P. Wijnheijmer, J. K. Garleff, K. Teichmann, M. Wenderoth, S. Loth, and P. M. Koenraad, Phys. Rev. B **84**, 125310 (2011).
[24] F. Marczinowski, J. Wiebe, F. Meier, K. Hashimoto, and R. Wiesendanger, Phys. Rev. B **77**, 115318 (2008).
[25] R. M. Feenstra, J. Vac. Sci. Technol. B **21**, 2080 (2003).
[26] A. Mang, K. Reimann, and St. Rübenacke, Solid State Commun. **94**, 251 (1995).
[27] W. R. L. Lambrecht, A. V. Rodina, S. Limpijumnong, B. Segall, and B. K. Meyer, Phys. Rev. B **65**, 075207 (2002).
[28] A. P. Ovchinnikow and B. M. Tsarev, Sov. Phys. Solid State **9**, 2766 (1968).
[29] D. E. Eastman, Phys. Rev. B **2**, 1 (1970).
[30] B. J. Coppa, C. C. Fulton, S. M. Kiesel, R. F. Davis, C. Pandarinath, J. E. Burnette, R. J. Nemanich, and D. J. Smith, J. Appl. Phys. **97**, 103517 (2005).
[31] D. C. Look, Surf. Sci. **601**, 5315 (2007).
[32] A. P. Wijnheijmer, J. K. Garleff, K. Teichmann, M. Wenderoth, S. Loth, R. G. Ulbrich, P. A. Maksym, M. Roy, and P. M. Koenraad, Phys. Rev. Lett. **102**, 166101 (2009).
[33] J. K. Garleff, A. P. Wijnheijmer, A. Yu. Silov, J. van Bree, W. VanRoy, J.-M. Tang, M. E. Flatté, and P. M. Koenraad, Phys. Rev. B **82**, 035303 (2010).
[34] We exclude that Zn hops between tetrahedral and octahedral interstitial sites because multiple changes [e.g., Fig. 1(d)] were observed. Moreover, calculations [35] predict that the tetrahedral site is unstable.
[35] A. Janotti and Ch. G. Van de Walle, Phys. Rev. B **76**, 165202 (2007).
[36] J. Ventura, J. B. Sousa, Y. Liu, Z. Zhang, and P. P. Freitas, Phys. Rev. B **72**, 094432 (2005).
[37] D. Solenov and K. A. Velizhanin, Phys. Rev. Lett. **109**, 095504 (2012).
[38] M. Blanco-Rey, M. Alducin, J. I. Juaristi, and P. L. de Andres, Phys. Rev. Lett. **108**, 115902 (2012).
[39] G. M. Dalpian and S.-H. Wei, Phys. Rev. B **72**, 075208 (2005).
[40] K. H. Chow and G. D. Watkins, Phys. Rev. Lett. **81**, 2084 (1998).